Microbial contributions to oxalate metabolism in health and disease

Menghan Liu[1,2], Joseph C. Devlin[1,2], Jiyuan Hu[1], Angelina Volkova[1,2], Thomas W. Battaglia[1], Allyson Byrd[3], P'ng Loke[1], Huilin Li[1], Kelly V. Ruggles[1], Aristotelis Tsirigos[1], Martin J. Blaser[4]*, Lama Nazzal[1]*

[1] NYU Langone Health, NY 10016, USA.

[2] Sackler Institute of Graduate Biomedical Sciences, NY 10016, USA.

[3] Department of Cancer Immunology, Genentech Inc., South San Francisco, CA 94080, USA.

[4] Center for Advanced Biotechnology and Medicine, Rutgers University, NJ 08854, USA.

* Correspondence to *martin.blaser@cabm.rutgers.edu* and *lama.nazzal@nyulangone.org*

Table of Contents

Abstract

Over-accumulation of oxalate in humans may lead to nephrolithiasis and nephrocalcinosis. Humans lack endogenous oxalate degradation pathways (ODP), but intestinal microbiota can degrade oxalate and protect against its absorption. However, the particular microbes that actively degrade oxalate *in vivo* are ill-defined, which restricts our ability to disentangle the underlying taxonomic contributions. Here we leverage large-scale multi-omics data (>3000 samples from >1000 subjects) to show that the human microbiota in health harbors diverse ODP-encoding microbial species, but an oxalate autotroph-*Oxalobacter formigenes*- dominates this function transcriptionally. Patients with Inflammatory Bowel Disease (IBD) are at significantly increased risk for disrupted oxalate homeostasis and calcium-oxalate nephrolithiasis. Here, by analyzing multi-omics data from the iHMP-IBD study, we demonstrate that the oxalate degradation function conferred by the intestinal microbiota is severely impaired in IBD patients. In parallel, the enteric oxalate levels of IBD patients are significantly elevated and associated with intestinal disease severity, which is consistent with the clinically known nephrolithiasis risk. The specific changes in ODP expression by several important taxa suggest that they play different roles in the IBD-induced nephrolithiasis risk.

Main

Oxalate is a two-carbon molecule broadly present in nature [1]. In humans, oxalate from dietary sources can be absorbed through the gastrointestinal tract or produced endogenously from hepatic metabolism, and chiefly excreted into the urine. Lacking endogenous oxalate-metabolizing enzymes, all mammals are vulnerable to oxalate toxicity, which manifests as nephrolithiasis, nephrocalcinosis, chronic kidney disease (CKD), and rarely as life-threatening systemic oxalosis [2-5]. Nephrolithiasis affect 8% of the US population [6, 7] with an ~20% 5-year recurrence rate [8, 9], and most kidney stones (85-90%) are composed of calcium oxalate[10]. Oxalate also has been implicated in inflammation and CKD progression, suggesting broad impact [11-14].

The mammalian intestinal microbiota can partially protect against oxalate toxicity by oxalate degradation [15-18]. Two recent large-scale epidemiological studies associated antibiotic use with increased nephrolithiasis risk [19, 20], presumably via a perturbed microbiota [21]. Multiple gut microbes can degrade oxalate [22], including *Oxalobacter formigenes*, an oxalate autotroph [23-27]. When given to animals, *O. formigenes* has reduced host oxalate burden [28-33]. *Escherichia coli*, *Bifidobacterium spp.* and *Lactobacillus spp.* also can degrade oxalate [34-43], but it is unclear which organisms are active oxalate degraders *in vivo*. A better understanding of human oxalate degrading microbes is needed to develop clinically protective strategies.

In particular, Inflammatory Bowel Disease (IBD) patients have heightened risk of oxalate toxicity due to elevated enteric oxalate levels and oxalate hyperabsorption, termed enteric hyperoxaluria (EH) [44-46]. Nephrolithiasis occurs in 12%-28% of adult IBD patients [44, 45]. Multiple factors are associated with EH in IBD patients, including lipid malabsorption and increased gut permeability. Another hypothesis is that microbiota-based oxalate degradation is impaired in IBD patients, leading to increased oxalate absorption [16].

Here, we leveraged large-scale multi-omics data to study oxalate degradation in the human microbiota. We curated all known microbial oxalate degradation pathways and identified those present in the human microbiota, and those that were transcriptionally active. We also interrogated the microbiota of IBD patients to understand shifts in microbiota-based oxalate degradation functions and their metabolic consequences.

Results

Type I and type II microbial oxalate degradation pathways (ODP)

To determine the ODP used by human gut bacteria, we curated all experimentally-validated microbial ODP from literature review and database searches (KEGG, MetaCyc, and Brenda) **(Fig. 1A)** [47-53]. There are two types of ODP based on their enzymatic mechanisms and co-factor requirements. Type I ODP cleave the oxalate carbon-carbon (C-C) bond in a single step **(Fig. 1A)** with no cofactor required**.** The two type I enzymes oxalate oxidase and oxalate decarboxylase **(Fig. 1A)** [54-57] are indistinguishable at the amino acid level [58] and belong to a single UniProt homologous protein family (IPR017774), therefore we refer to them jointly as oxalate oxidase/decarboxylase (OXDD). Type II ODP consists of two enzymatic reactions requiring coenzyme A as co-factor **(Fig. 1A)**. Initially, coenzyme A is added to oxalate to form oxalyl-CoA, e.g. by formyl-CoA transferase (FRC) **(Fig. 1A)**. In the second step, all type II ODP use oxalyl-CoA decarboxylase (OXC) to metabolize oxalyl-CoA into CO_2 and formyl-CoA **(Fig. 1A)**.

As such, we then acquired all available protein homologs of OXDD (n=2836), FRC (n=1947), and OXC (n=1284) from UniProt Interpro [59, 60]. By tracing the taxonomic origin of the genes encoding those homologs, we found that OXDD-coding taxa can be fungal or bacterial, whereas FRC- and OXC-coding taxa are strictly bacterial **(Fig. 1B)**. The frequent co-occurrence of FRC and OXC in individual genomes indicates encoding complete type II ODPs **(Fig. 1B)**. As expected, OXDD, FRC, and OXC each are conserved within the same microbial class, but

exhibit substantial divergence across individual classes **(Fig. S1)**. These data provide a comprehensive overview of ODP pathways and a reference set of ODP-encoding microbes, which enable analyses to elucidate those relevant to humans.

Type II ODP are utilized by the gut microbiota of healthy humans

Next, we ask which of these ODP are encoded and expressed within the metagenomes and metatranscriptomes of healthy humans **(Fig. S2)**. Multi-omics data from five studies were selected for downstream analyses, collectively including 2359 metagenome samples and 1053 metatranscriptome samples from 660 and 165 subjects, respectively **(Fig. S2, Table S1)**. After removing host-associated and low-quality reads, using DIAMOND Blastx [61] all remaining sequences were compared with the unique oxalate-degrading enzyme (ODE) homologous proteins, including 2519 OXDD, 1556 FRC, and 1037 OXC homologs. Alignment pairs with identity > 90% were retained for downstream analyses; this cut-off was determined by the protein identity of the inter- and intra-species ODEs to be robust for distinguishing ODEs that originated from different microbial species **(Fig. S3)**.

We found that ODEs were ubiquitously harbored in the healthy gut microbiome; at least one ODE was detected in the metagenome of 607 (92%) of the 660 subjects examined, and in the metatranscriptome of 132 (80%) of the 165 subjects available. In the metagenomes, the type II ODE FRC- and OXC-encoding genes *frc* and *oxc* were substantially more prevalent **(Fig. 2A)**, and more abundant **(Fig. 2B)** than the type I ODE OXDD-coding gene *oxdd*. Similarly, in the metatranscriptomes, *frc* and *oxc* expression also were substantially more prevalent **(Fig. 2C),** and abundant **(Fig. 2D)** than *oxdd* expression. These findings were consistent in all studies, despite differences in source populations and sample preparation methods **(Table S1)**. In addition, specific *frc* and *oxc* genes **(Fig. S4)** were frequently co-expressed within the same microbiota, indicating the expression of the complete type II ODP. In total, these data indicate

that the human microbiome is commonly and predominantly composed of microbes utilizing type II rather than type I ODP. As such, we focused on the type II ODP for the remaining analyzes.

ODPs are encoded by multiple microbes, but dominantly expressed by *Oxalobacter formigenes* in healthy human microbiota

Although multiple microbes are known to encode *frc* and *oxc* [22, 62-64], their functional activity *in vivo* has not been studied. We next systematically characterized the active oxalate degraders *in vivo* by searching for the microbial species that transcribe these type II ODP genes. In the metagenome of 660 healthy subjects, we detected *oxc* encoded by multiple human gut microbes including *E. coli, O. formigenes, Muribaculaceae sp, and several Bifidobacterium sp.*, *Lactobacillus sp*, **(Fig. 3A, left)**, some of which have been reported to degrade oxalate [31, 34-37, 41-43, 62, 65, 66]. The abundance of *oxc* of those species varied widely (median RPKM of 0.006-0.223) **(Fig. 3A, left).** The most prevalent oxc-encoding microbe was *E. coli* (*oxc* detected in 56% of subjects), followed by *O. formigene*s (*oxc* detected in 39%). The abundance and prevalence pattern for *oxc* was consistent across different studies **(Fig. S5, S6)**, and was parallel to the other type II ODE *frc* **(Fig. S7),**

Surprisingly, *oxc* expression across species did not directly correlate with *oxc* metagenomic abundance or prevalence **(Fig. 3A, right)**. For *O. formigenes*, whose growth relies on oxalate degradation [23, 67, 68], *oxc* expression was both most abundant and most prevalent, present in the metatranscriptome of 61% of subjects **(Fig. 3A, right)**. In contrast, *E. coli oxc* expression was observed in only 12% of subjects **(Fig. 3A, right)**, despite gene presence in 56% of subjects **(Fig. 3A, left).** For *Bifidobacterium* and *Lactobacillus* species, whose oxalate degradation activity was reported *in vitro* and in animal models [42, 43, 66], *oxc* expression was observed at low prevalence (< 5%), or not observed at all (*B. pseudocatenulatum*, *B. choerinum*)

153 **(Fig. 3A right)**. Collectively, these data demonstrate variation in the extent of ODP transcription
154 by species and individual hosts.

155 To test the species-specific expression pattern of ODP in a more rigorous manner, we restricted
156 our analysis to the subject-matched metagenome and metatranscriptome that derived from the
157 same microbiota communities **(Fig. 3B)**. *O. formigenes* ODP expression was observed in most
158 subjects whose microbiome harbored the corresponding gene **(Fig. 3B)**, and in many subjects
159 in whom the gene was not detected, indicating underdetection of *O. formigenes* ODP at the
160 genomic level. In contrast, *E. coli* ODP expression was only observed in a small portion of
161 subjects harboring the corresponding genes **(Fig. 3B)**. The relative lack of detection of *O.*
162 *formigenes* ODP genes in the metagenomic data may reflect the highly variable abundance of
163 the organism itself falling at times below the lower limit of detection using genetic-based
164 methods [69-72].

165 We then assessed population-level contribution (see Methods) to quantify the impact of
166 individual species on global ODP. The contribution of *O. formigenes* to ODP increased from 17%
167 to 63% from the metagenomic to the metatranscriptomic level, greater than the transcriptomic
168 contributions of all other species combined **(Fig. 3C, Table S2)**. Conversely, the contribution of
169 *E. coli* to ODP was markedly reduced from the metagenomic (36%) to the metatranscriptomic
170 (7%) level **(Fig. 3C)**. The contributions of other species to ODP at the metagenomic and
171 metatranscriptomic levels varied, but none were dominant **(Fig. 3C)**. A parallel pattern was
172 observed for *frc* **(Fig. S8, Table S3)**. Network analysis did not yield significant species-species
173 interactions related to *oxc* transcription, potentially because the activity of non-*O. formigenes*
174 species was too low across the studies (data not shown).

175 In summary, we systematically described the gut microbes responsible for oxalate degradation
176 *in vivo* in health, showing that this microbial function is dominated by a single species-*O.*
177 *formigenes*. These data provide a baseline for examining the disease-associated changes in
178 subsequent analyses.

Impaired microbiota-based oxalate degradation and elevated enteric oxalate levels in IBD patients

IBD patients frequently suffer from Enteric Hyperoxaluria (EH), with oxalate hyperabsorption and formation of calcium oxalate kidney stones [44-46]. In particular, Crohn's disease (CD) with ileocolonic involvement is associated with greater nephrolithiasis risk compared to either ileal or colonic involvement alone [73]; Ulcerative colitis (UC), regardless of severity and location, is associated with stone formation [73]. We hypothesized that the oxalate degradation function conferred by the intestinal microbiome may be impaired in IBD patients, ultimately leading to more intestinal and circulating oxalate in the host. To address this question, we acquired the multi-omics iHMP-IBD study data [74, 75] to assess both oxalate homeostasis and microbiota-based oxalate degradation.

We stratified the iHMP-IBD patients into UC (N=30), CD (N=54) groups, regardless of the disease location, and a CD subgroup with the ileocolonic phenotype at baseline - CD-L3 (n=25). Consistent with the clinical nephrolithiasis risk, fecal oxalate concentrations were elevated in both the UC patients (p=0.005) and CD-L3 patients (p<0.001) compared to healthy controls; the same trend was observed in the CD patients (p=0.06) **(Fig. 4A)**. Fecal oxalate was most increased in the CD-L3 patients **(Fig. 4A, Fig. S9)**. We also examined the differences in fecal oxalate concentrations in a linear mixed-effects model, adjusted for subject age, and sex as fixed effects and repeated measurements as a random effect, and observed the effects at marginal levels (p=0.095 for CD, p=0.083 for UC, p=0.058 for CD-L3).

Expression of *frc* in the gut microbiota was only observed in 50% of UC (p<0.05), 65% of CD and 64% of CD-L3 patients compared to 76% in healthy subjects **(Fig. 4B)**, and the levels of expression were significantly decreased in all IBD groups (p<0.001) **(Fig. 4C)**. Similarly, *oxc* expression was observed in 57% UC, 54% CD and 48% CD-L3 patients **(Fig. 4B)** compared to 71% in healthy persons, and was significantly downregulated in the UC group (p<0.001) **(Fig.**

4C). Type I ODE *oxdd* was rarely observed in the IBD microbiota, similar to healthy persons (data not shown).

We then asked whether there was a relationship between the decreased microbiota-based ODP expression and oxalate levels in the intestinal tract. By Spearman correlation, 44%-57% of the variance in fecal oxalate could be explained by variation in ODP expression in IBD patients ($p<0.05$ for UC and CD-L3 subjects) **(Fig 4D)**. In contrast, microbial ODP genes showed increased abundance in IBD patients **(Fig. S10 A, B)**, indicating the discrepancies between the gene abundance and expression levels.

Collectively, these data indicate that IBD patients have decreased microbiota-based oxalate degradation; the observed elevated intestinal oxalate may be a consequence, conferring increased susceptibility to EH.

Loss of *O. formigenes* and downregulation of its ODP in IBD patients

We next sought to identify which microbial species accounted for the reduced ODP expression in IBD patients. The two species *E. coli* and *O. formigenes* with the largest ODP contributions at the genomic and transcriptional level, respectively, were notable.

Using gene and transcript jointly as markers, ODP expression by *O. formigenes* was detected in only ~25% in UC and in CD patients **(Fig. 5A)** - less prevalent than the ~70% in healthy individuals, either when studies were combined **(Fig. 5A)** or separate **(Fig. 3D)**. Having the lowest *O. formigenes* prevalence, the CD-L3 group had strongest negative correlation between fecal oxalate and expression of *oxc* **(Fig. 4D)**. Consistent with the low prevalence, the ODP expression by *O. formigenes* was also less abundant in UC, CD, and in CD-L3 patients compared with controls ($p<0.01$ for all groups), marked by lower RPKM values **(Fig. 5B)**, Interestingly, *O. formigenes* ODP was always actively expressed, when genes were observed, within the microbiota of the IBD subjects **(Fig. 5A).** In contrast, the ODP of *E. coli* was detected

in nearly all IBD subjects and was transcribed more frequently compared to healthy subjects **(Fig. 5A)**.

In total, these data revealed the complex pattern of taxa-specific ODP expression change during a disease state. In particular, the contrasting patterns of *O. formigenes* and *E. coli* illustrate the varied responses in association with distinct disease progression. Abolishing the ODP expression of *O. formigenes*, leads to the impaired global oxalate degradation, which further leads to increased circulating oxalate. Although *E. coli, Lactobacillus* spp*,* and *Bifidobacterium* spp, use their ODPs to defend against oxalate-induced acid stress [34, 41, 62, 64, 66], their upregulated ODP in IBD is a secondary response to the elevated oxalate levels present.

Discussion

Oxalate degradation by the human microbiota has been known since the 1940s [15, 17, 18, 49, 68, 76, 77], but the taxa involved *in vivo* were not clear [78, 79]. We present the first comprehensive study of human oxalate-degrading microbes, with multi-omics evidence, and quantitatively characterized their contributions. Our finding that multiple human gut microbes encode ODPs is consistent with multiple prior studies [22, 43, 64, 80, 81], but surprisingly, oxalate degradation in the gut microbiome was dominated by a single organism - *O. formigenes*, which is the only known oxalate-degrading specialist that exclusively uses oxalate as energy and growth sources [22]. By actively transcribing ODPs, *O. formigenes* dominates the global ODP of the microbiota, consistent with a previous proteomic analysis of *O. formigenes* cells, showing FRC and OXC as the most abundant proteins produced during exponential and lag stages [82].

Most kidney stones (85-90%) are idiopathic with few genetic associations [83]. Here using the risk population for nephrolithiasis – IBD patients as the surrogate, we provide novel insights that the impaired metabolic activity of the microbiota may mediate enteric oxalate levels and nephrolithiasis risk. We showed that fecal oxalate concentrations were elevated in the iHMP-IBD UC patients, and CD patients with ileocolonic involvement, which is consistent with the clinical observations of high EH risk [73, 84, 85]. EH may be an attractive indication for *microbiota*-associated therapy, as the elevated soluble oxalate is in the intestine, providing an advantage for oxalate degrading bacteria, such as *O. formigenes* to colonize and to be metabolically active. Our finding that *O. formigenes* is less common in IBD patients than in healthy individuals provides a rationale for restoring *O. formigenes* in this population. Previously *O. formigenes*-related therapeutics was only examined in patients with primary hyperoxaluria (PH) and yielded inconsistent results [28, 29, 86, 87]. In contrast to EH, PH is caused by high circulating oxalate of host origin, therefore *O. formigenes*-based therapy may be limited by oxalate secretion into the intestinal lumen [31, 88, 89] for direct bacterial access.

The contrasting genetic and transcriptional changes in ODP observed in this study highlight the importance of evidence beyond the gene level for microbiome studies. The integrative multi-omics analysis framework built for this study, now deposited on Github, can also be extended to a broad range of microbiome functions of interest, such as choline and tryptophan metabolism, for example.

Methods

Meta-omics data of the human microbiome. Metagenomic and metatranscriptomic data of healthy human subjects were collected from 5 studies and 4 studies, respectively[75, 90-95]. Metagenomic and metatranscriptomic data of healthy humans and IBD subjects were collected from the iHMP-IBD study [75]. Each sample was cleaned by KneaData to remove low-quality

reads and host-associated reads. The metabolic profiles of each sample were surveyed using HUMAnN2 v0.11.1 [96] under parameters *--prescreen-threshold 0.01, --pathways-database metacyc_reactions_level4, metacyc_pathways_structured* and *--protein-database uniref50*, for the comparison in **Fig. S2.** Fecal oxalate concentration was determined from untargeted metabolomics data from iHMP-IBD; measurements related to oxalate were selected for analysis.

Homologous proteins of ODE. The homologs protein families of OXDD, FRC, and OXC were characterized by UniProt Interpro [59, 60] (V70) in protein families IPR017774, IPR017659, and IPR017660, respectively. We acquired the taxonomic origin and amino acid sequences of 2,699 OXDD, 1,947 FRC, and 1,284 OXC homologs. Protein homologs that are 100% identical were then de-duplicated into 2519 OXDD, 1556 FRC, and 1037 OXC unique homologs, which were used as a reference database of ODEs for a subsequent query against the meta'omics data. Oxalate oxidoreductase **(Fig. 1A)**, a recently discovered enzyme with limited information [51, 52, 97-101], was not considered in this present study.

Pairwise identity between ODE protein homologs. Multiple sequence alignments were performed among the 2519 OXDD, 1556 FRC, and 1037 OXC unique protein homologs separately, by muscle [102] in seaview v4.7 [103]. The alignments then were trimmed and imported into R. The pairwise alignment distance d was calculated using function *dist.alignment* in the seqinR package [104] based on identity or Fitch matrix [105]. The alignment distance d was subsequently converted to percent protein identity $100 * (1 - d^2)$, following the documentation of *dist.alignment*.

Detection of ODE in the meta'omics data. The quality-filtered meta'omics data were aligned against the reference protein databases consisting of 2519 OXDD, 1556 FRC, and 1037 OXC unique homologs, by diamond blastx [61], with best hit returned (--max-target-seqs 1). Alignments with identity > 90% were kept for downstream analysis to achieve species-level resolution for most taxa **(Fig. S3)** The abundance of each ODE protein homolog was calculated

as reads per kilobase per million (RPKM) in each sample. When multiple timepoints were available, each subject was represented by the mean measurements across all samples provided.

Population-level contribution to ODE. The population-level contribution of a species to ODE was designed as a measurement to take both prevalence and abundance information into consideration. It is calculated for each ODE separately, based on their abundances (RPKM values).

Using oxc as the example, suppose there are M *oxc*-coding species and N samples. In any given sample j, the contribution of species i to OXC, c_{ij}, is represented by its relative oxc abundance, calculated from

$$c_{ij} = z_{ij} / \sum_{i=1}^{M} z_{ij}$$

where the z_{ij} denotes the $RPKM_{oxc}$ of species i in sample j. In this way, we normalize across samples with the total contribution in any OXC-positive samples is fixed to 1, in any OXC-negative samples is 0.

The population-level contribution of species i: C_i, can be subsequently calculated from summating contribution of species i in N samples, as follows

$$C_i = \sum_{j=1}^{N} c_{ij}$$

Note that population-level contribution of species monotonically increases with sample size N. Therefore, it is transformed to relative scale when being compared across different populations or different sample types (metagenome vs. metatranscriptome), such as in **Fig. 3C**, **Fig. S8,** and **12**.

Network analysis. A network analysis on *oxc* or *frc* expression from microbial species using SpiecEasi[106]. The raw RPKM values were used and the networks were constructed under default parameter *method='mb', sel.criterion='bstars', lambda.min.ratio=2e-2,nlambda=100, pulsar.params=list(rep.num=20, ncores=2)*.

Code availability. Source code of the pipeline can be found on Github via https://github.com/ml3958/FindTaxaCtrbt. Downstream analyses scripts are available per request.

Acknowledgements

We thank Dr. David Goldfarb, Dr. David Fenyo, Dr. Victor Torres, Dr. Joao Xavier and Xuhui Zheng for their helpful comments. This study was supported in part by U01AI22285, R01DK110014, and the Rare Kidney Stone Consortium (U54 DK083908) from the National Institutes of Health, by the C & D and Zlinkoff Funds, Oxalosis and Hyperoxaluria Foundation-American Society of Nephrology career development grant, and the TransAtlantic Partnership of the Fondation LeDucq.

Contributions

M.L, L.N, and M.J.B designed the study and wrote the manuscript. M.L, J.C.D, J.H performed the analyses. M.L, J.C.D, A.V, T.B collected the data. A.B, P.L, H.L, K.V.R, A.T contributed by suggesting additional new analysis and associated methods.

Competing interests

A.L.B is an employee of Genentech. The remaining authors have no competing interest.

345

Figures

Figure 1.

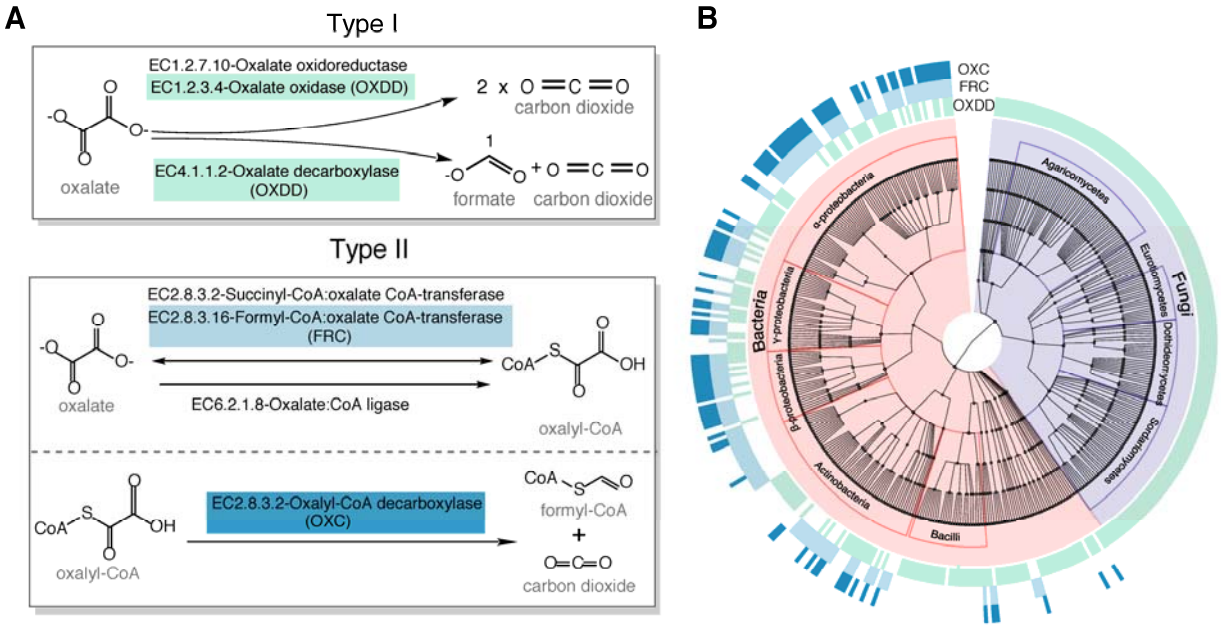

Figure 1. Type I and type II microbial oxalate-degrading pathway (ODP).

(A). Schema of type I and type II ODP. Enzymes are annotated with corresponding KEGG IDs. OXDD, FRC, and OXC are the focus of the present study.

(B). Cladogram of microbial genera that encode oxalate-degrading enzymes OXDD, FRC, and OXC. The three rings surrounding the cladogram indicate OXDD-, FRC- or OXC-encoding genera, respectively.

Figure 2.

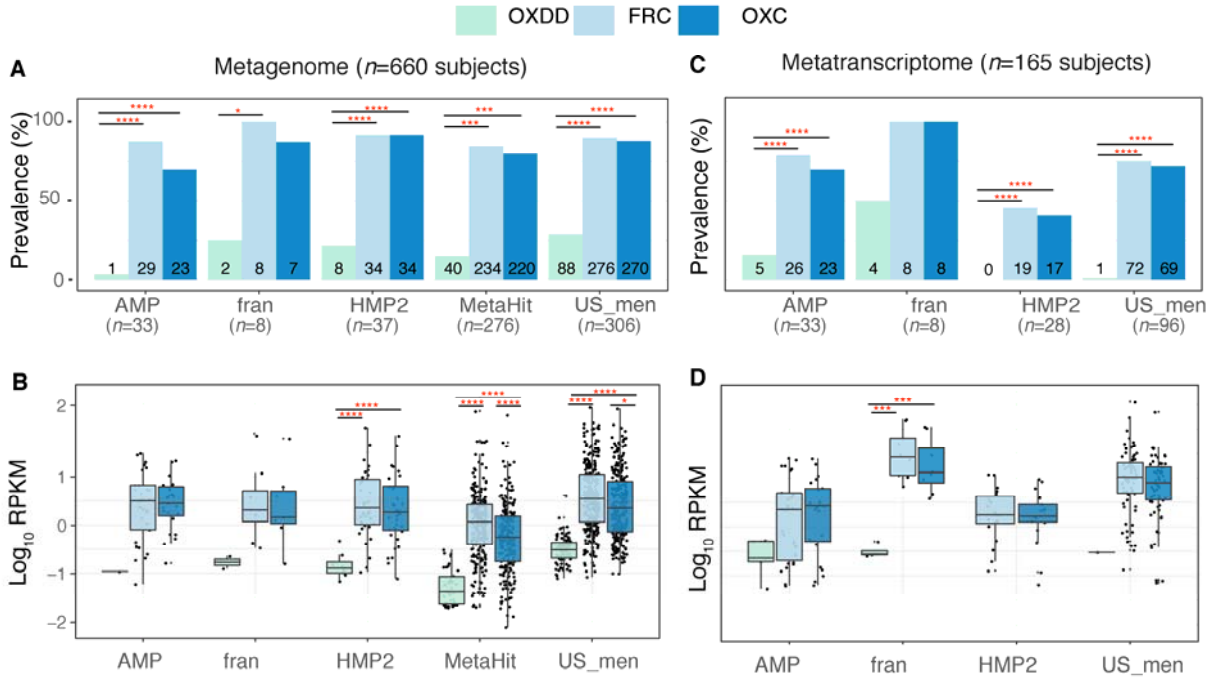

Figure 2. Detection of type I and II ODE within the fecal metagenome and metatranscriptome of 660 and 165 healthy human subjects.

Prevalence (A) and abundance (B) of ODE in the fecal metagenome of five studies surveyed. Numbers written on the bottom bars indicate the numbers of subjects in whom the corresponding ODE is detected, and only those subjects were considered in panel B.

Prevalence (C) and abundance (D) of OXDD, FRC, and OXC in the fecal metatranscriptome of four studies surveyed.

*: p< 0.05, **: p< 0.01, ***: p< 0.001, ****: p< 0.0001, by proportion tests for panels A and C, by multiple-adjusted Mann-Whitney tests for panels B and C.

Figure 3.

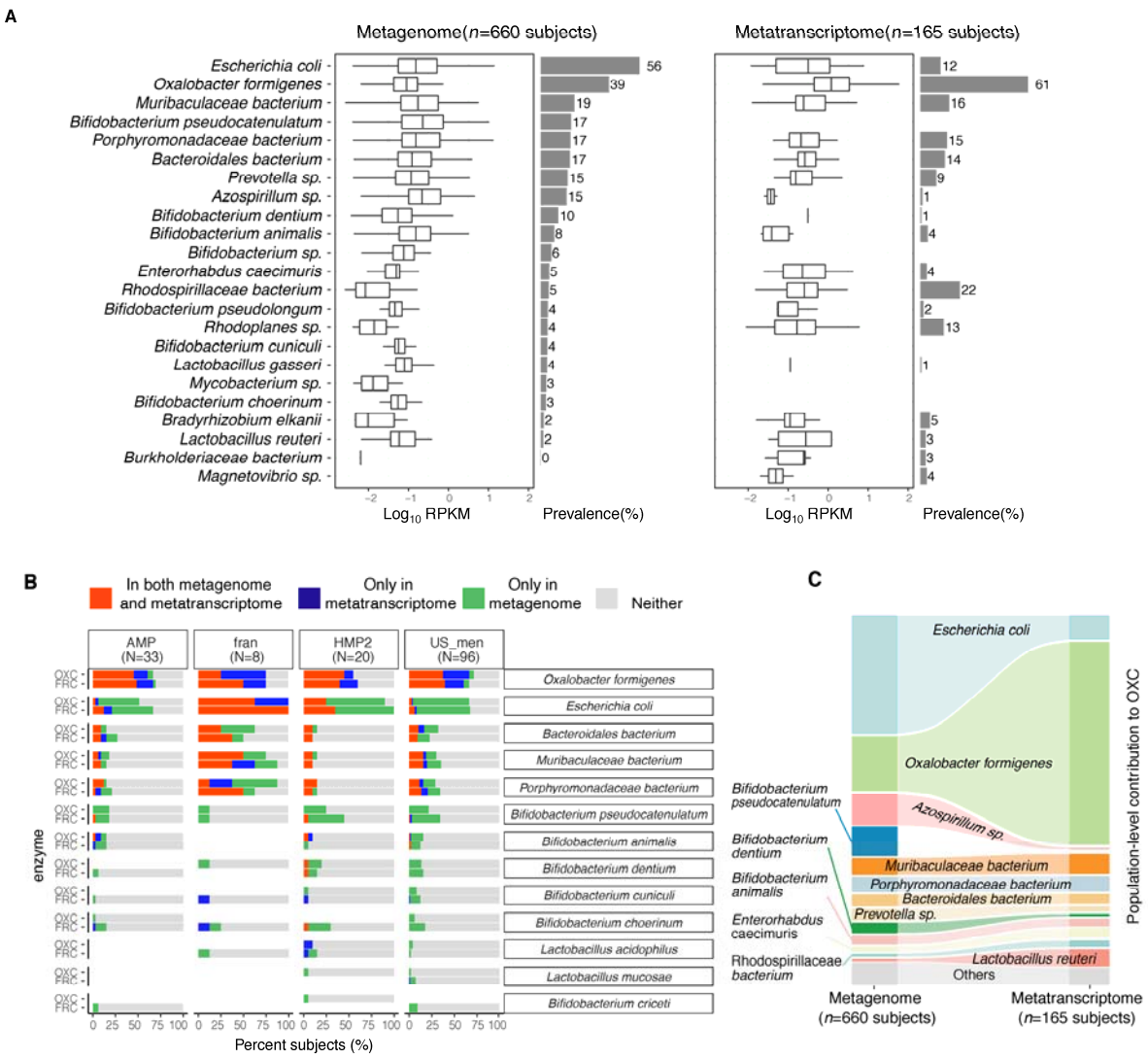

Figure 3. Expression of type II ODP of microbial species within the intestinal microbiota of healthy humans.

(A) Abundance and prevalence of OXC of microbial species in the metagenome (left) or metatranscriptome (right) of 660 and 165 subjects. Box plots indicate the abundance of microbial OXC ($\log_{10}$ RPKM) among subjects in whom OXC is detected, and are generated with *ggplot2* with outliers excluded. Bar plots indicate the prevalence of microbial oxc, with percentage annotated. Microbial species are ordered by the corresponding metagenomic OXC prevalence. A parallel analysis for FRC is shown in Suppl. Fig 5.

(B) Detection of OXC and FRC of microbial species in the subject-matched metagenome and metatranscriptome, by study. For each microbial ODE, the subjects are divided into four groups (shown in different colors) based on the co-detection of ODE in the matched metagenome and metatranscriptome, with percent (%) of which reflected. The fran Study, from which *E. coli* ODP was detected in all subjects, used a sample extraction method known to induce *E. coli*, as noted in their publication [92].

(C). Population-level contribution of individual species to metagenomic (left) or metatranscriptomic (right) OXC. The population level-contribution of each species was calculated at a relative scale (see Methods) and plotted. Raw values can be found in Suppl. Table 1. The 10 species that

have the highest metagenomic or metatranscriptomic contribution are shown. A parallel analysis for FRC is shown in Suppl. Fig. 7.

Figure 4.

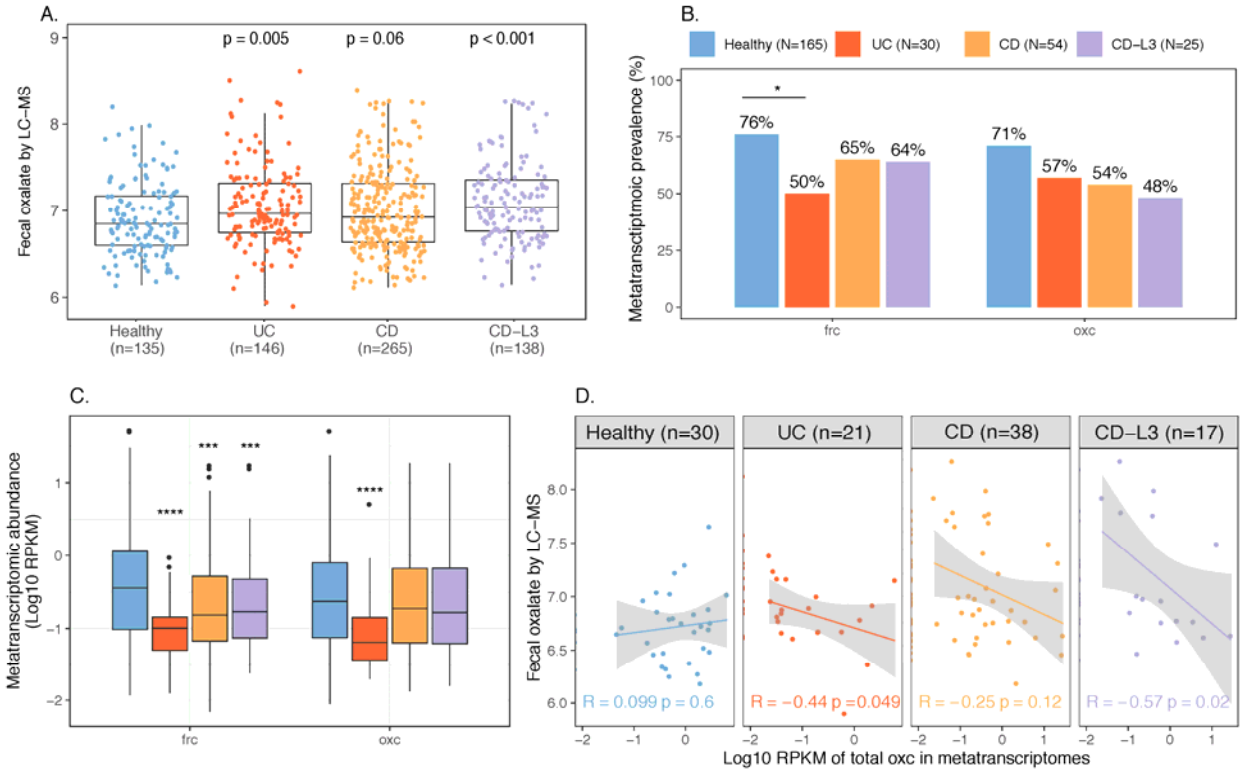

Figure 4. Elevated fecal oxalate concentrations and reduced expression of microbiome ODP in IBD patients.

(A). Stool oxalate concentrations in healthy, UC, CD, or CD-L3 subjects from HMP-IBD study. L3 refers to the ileocolonic phenotype, according to the Montreal Classification) at baseline. Data derived from iHMP-IBD untargeted metabolomics measurements.

Prevalence (B) and abundance (C) of OXDD, FRC, and OXC in metatranscriptomes of healthy, UC, CD, or CD-L3 subjects. The 165 healthy controls are combined from four studies (AMP, US_men, fran, HMP2). *: p< 0.05, **: p< 0.01, ***: p< 0.001, ****: p< 0.0001 by multiple-adjusted Mann-Whitney tests in A and C, by proportion test in B. (D). Spearman correlations of fecal oxalate and total metatranscriptomic OXC. Spearman Rho and p values are shown.

Figure 5.

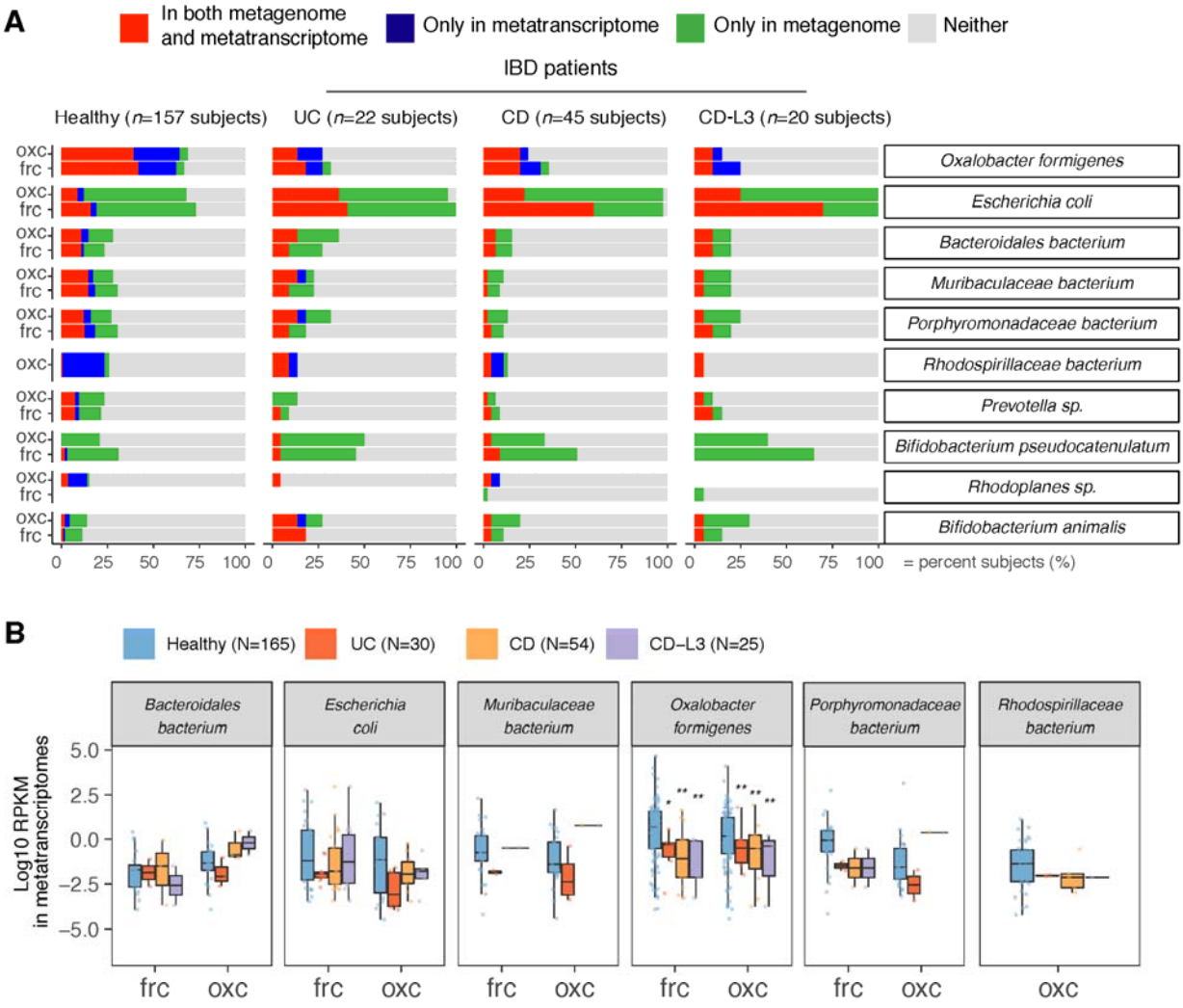

Figure 5. Differential ODP expression by human gut microbes in healthy and disease states.

(A) Detection of microbial OXC and FRC in the subject-matched metagenome and metatranscriptome from healthy subjects, UC, CD, or CD-L3 patients. For each species shown, the subjects are divided into one of four categories based on the co-detection of ODE in the matched metagenome and metatranscriptome.

(B) Expression of microbial FRC and OXC in the metatranscriptomes of healthy subjects, UC, CD, or CD-L3 patients. Boxplot reflects the subjects, in whose metatranscriptome the corresponding enzyme is detected. * p <0.01, ** <0.0001 by multiple-adjusted Mann-Whitney tests.

Supplementary Figures

Figure S1.

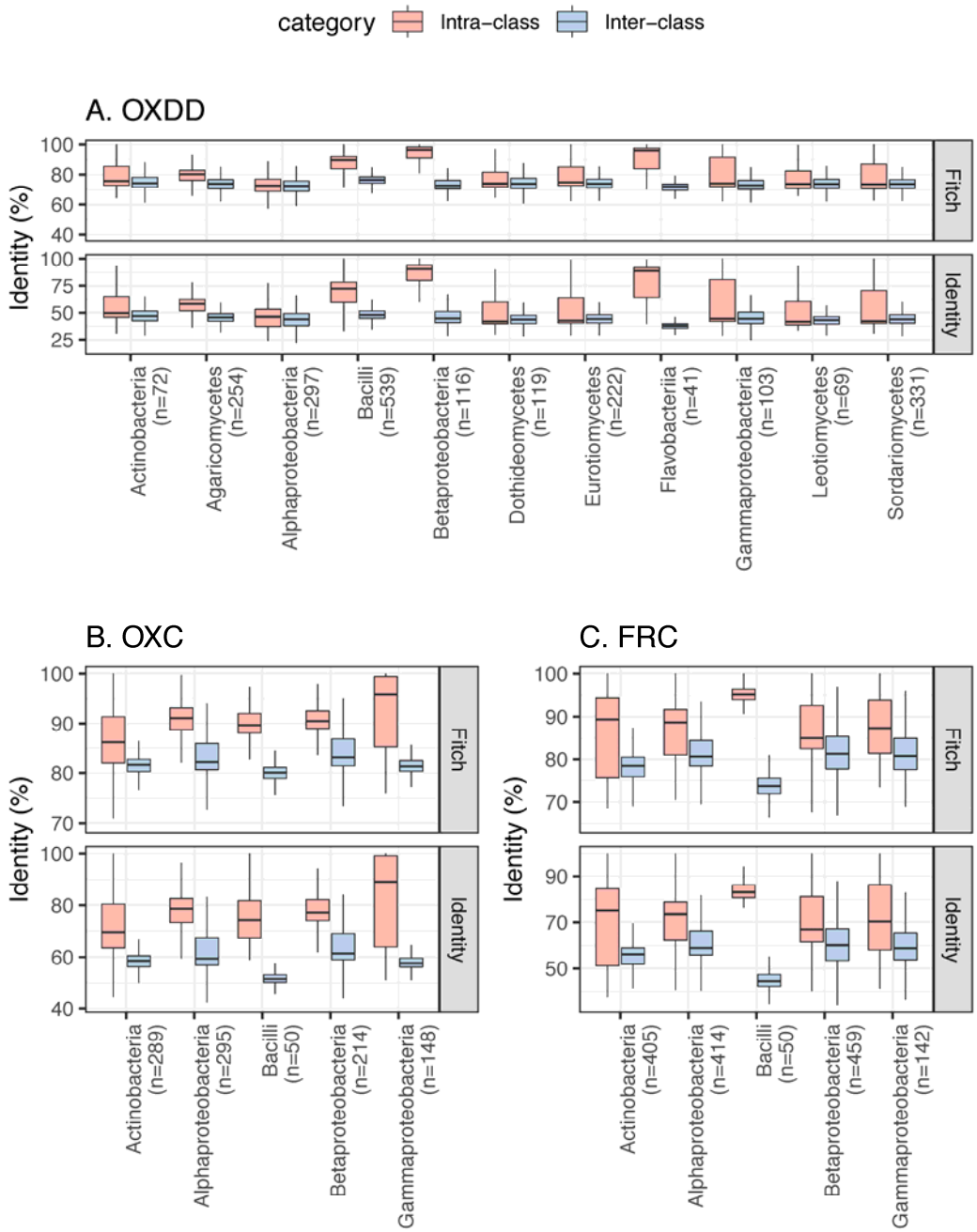

Figure S1. Inter-class and intra-class ODE protein identity associated with each microbial class. Panels focus on OXDD **(A)**, OXC **(B)**, or FRC **(C)**. The pairwise identity between any two protein homologs was calculated based on the multiple alignments using amino acid sequences, by Fitch [105] or identity distance matrix (See Methods for details). The number of ODE homologs available for each class is indicated in parenthesis. Classes with >20 ODE are shown.

Figure S2

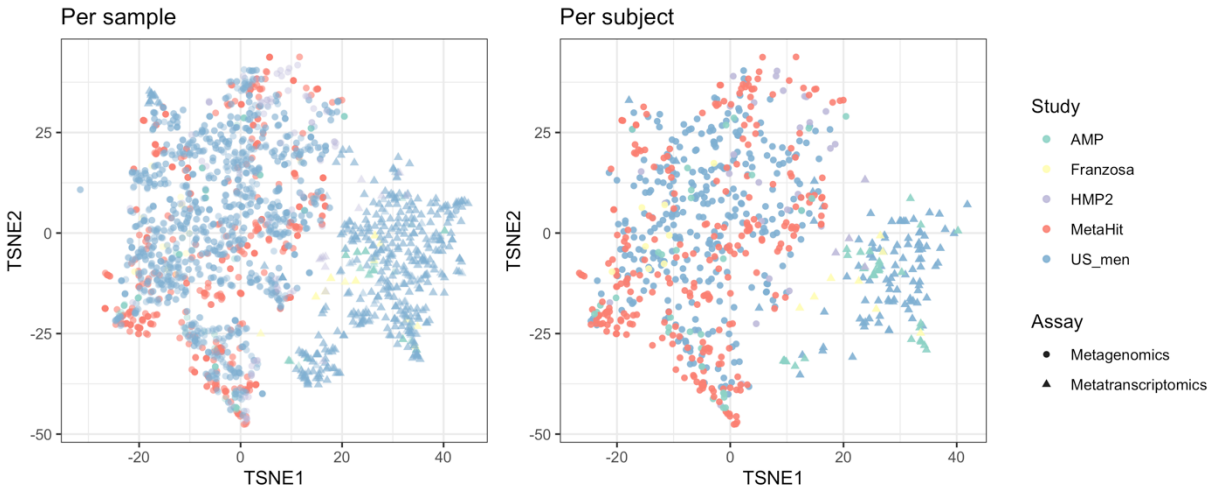

Figure S2. Beta-diversity of metabolic profiles associated with the metagenomic and metatranscriptomic samples from healthy human subjects, ordinated on a Tsne (t-distributed stochastic neighbor embedding) plot. The metabolic profile is assessed by the HUMAnN2 [96] pipeline using (see Methods). The metabolic profiles for each subject are calculated by taking the mean measurements provided. The table shows the number of subjects who provided metagenomic (MTG ●) and metatranscriptomic (MTS ▲) data. See **Table 1** for study information.

510 **Figure S3.**

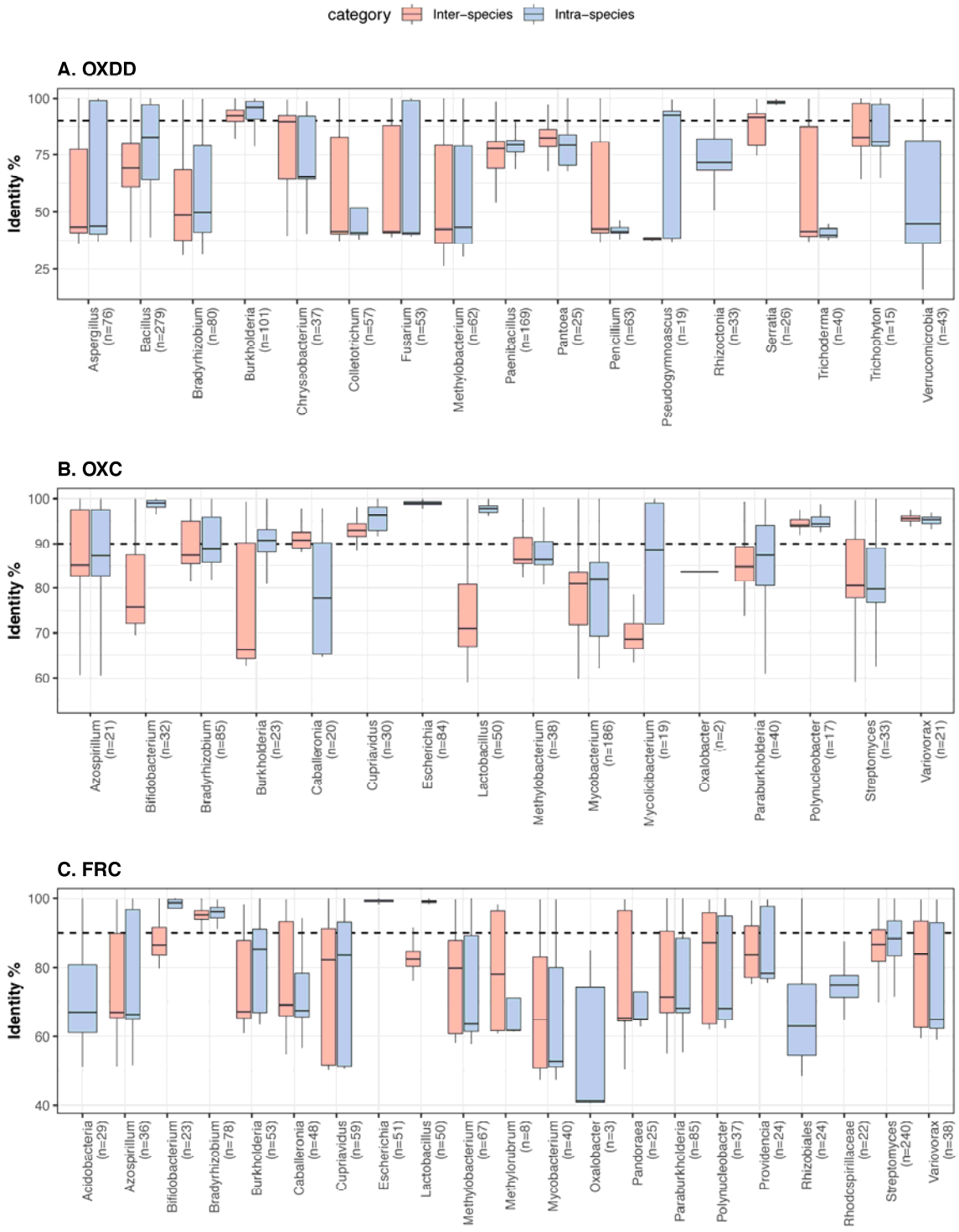

511

512 **Figure S3. The protein identity between inter-species and intra-species ODEs, for each microbial**
513 **genus.** Panels focus on OXDD(A), OXC (B), or FRC (C)**.** The pairwise protein identities were calculated
514 based on amino acid sequence alignment (See Methods for details). The number of ODE homologs
515 available for each genus is indicated in parenthesis. The blastx identity cutoff 90% used in this study is
516 indicated by the dashed line. Genera with >20 ODE homologs and Genus *Oxalobacter* are shown.

517

518 **Figure S4**

519

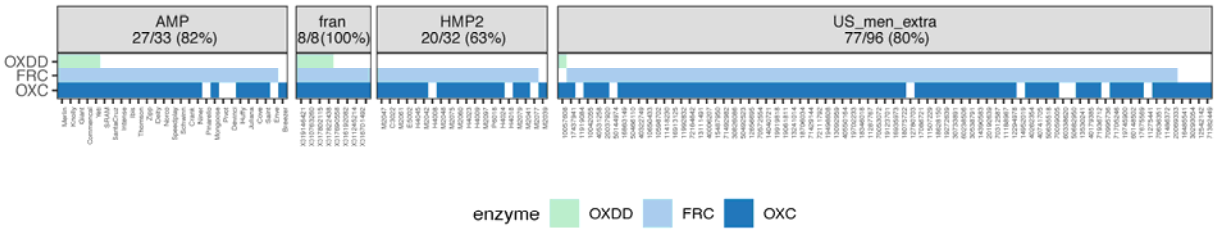

520

521 **Figure S4. Co-detection of OXDD, FRC, and OXC in the metatranscriptomes of subjects across**
522 **different studies.** Subjects with at least one ODE detected in the metatranscriptome are shown, with
523 percent of total subjects displayed in panels, for each study, indicated in parentheses.

524

Figure S5

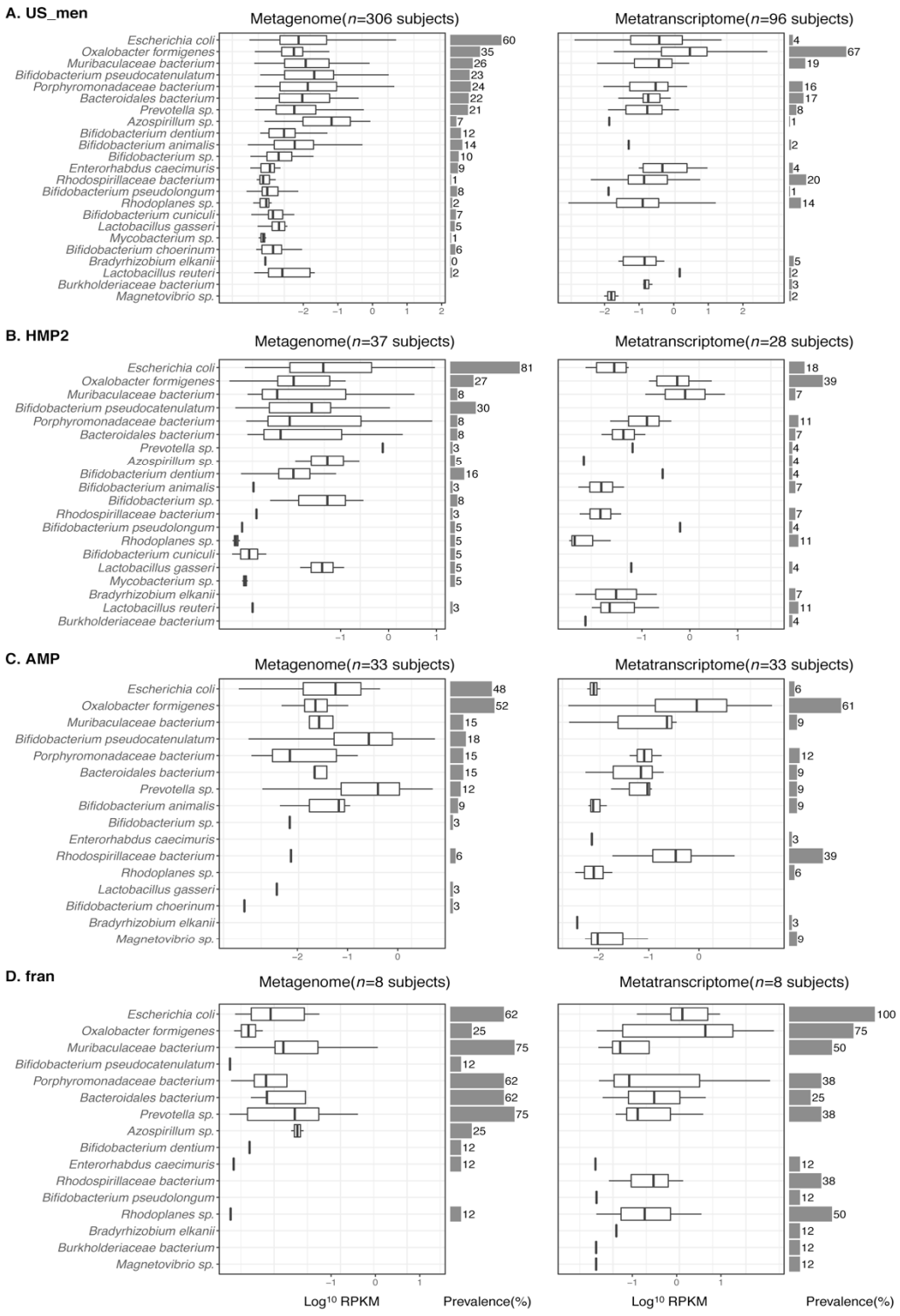

Figure S5. Detection of OXC of microbial species in the microbiome of healthy human subjects from US_men (A), HMP2 (B), AMP (C), or fran (D) study. Left and right panels focus on detection in metagenomic and metatranscriptomic data, respectively. (Follows legend of **Fig. 3A**).

562 **Figure S6**

563

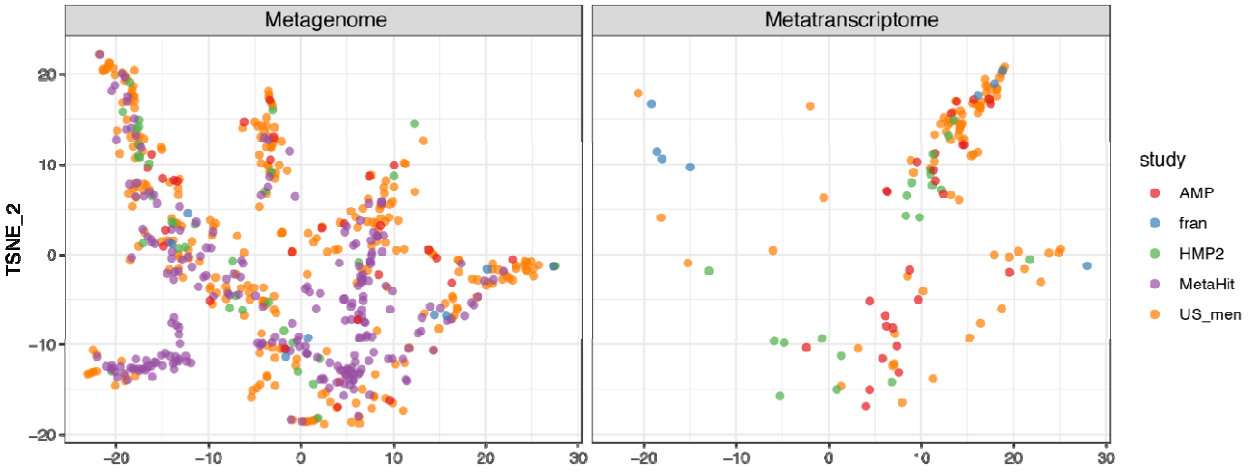

564

565

566 **Figure S6. Tsne plot of 594 metagenomic and 131 metatranscriptomic samples, based on the**
567 **abundances OXC and FRC**. OXC and FRC of microbes in **Figures 3A and S5** were used. Tsne is
568 calculated with *Rtsne v0.15* package in R. The OXC- and FRC- specific study effects are not significant,
569 examined using PERMANOVA using 1000 permutations (p>0.1).

570

571 **Figure S7**

572

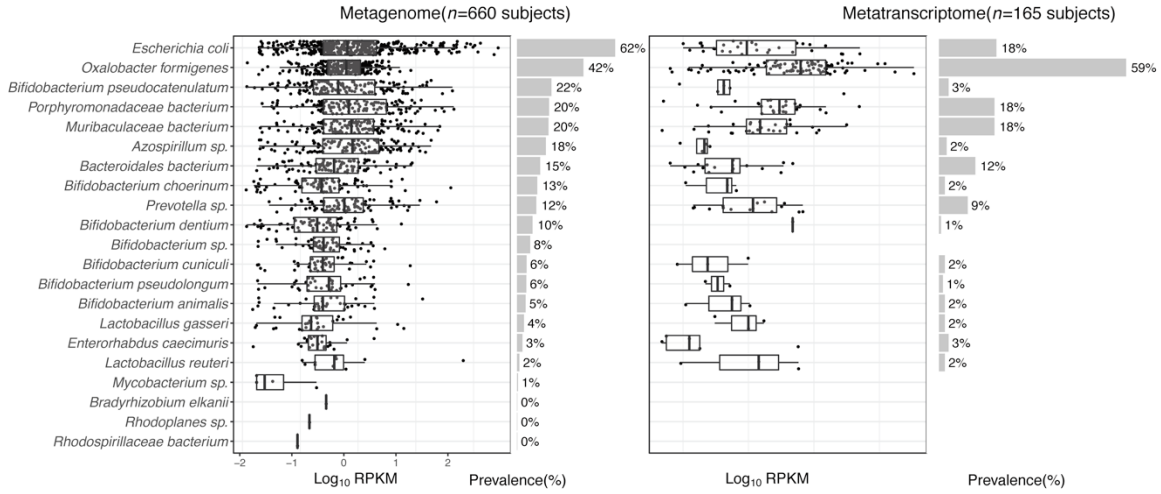

573

574

575

576 **Figure S7. Detection of FRC of microbial species in the metagenome (left) or metatranscriptome**
577 **(right) of healthy human subjects.** (Follows the legend of **Fig. 3A**).

578

579

580

Figure S8

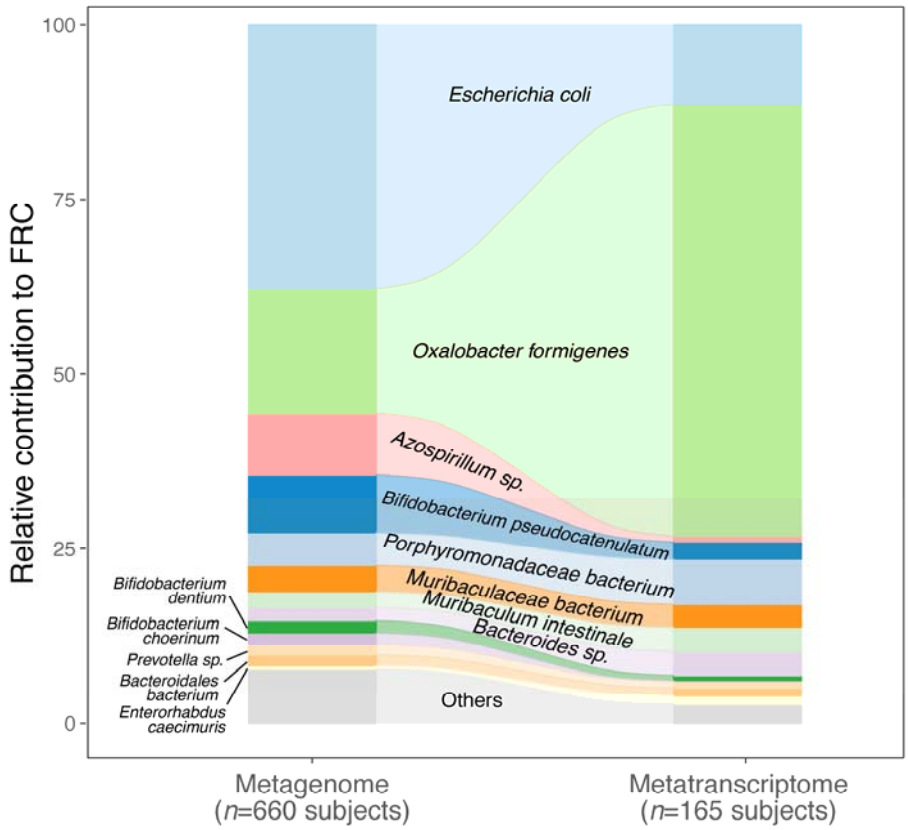

Figure S8. Population-level contribution of individual species to metagenomic (left) or metatranscriptomic (right) FRC. Follows the legend of **Fig. 3D**.

605 **Figure S9**

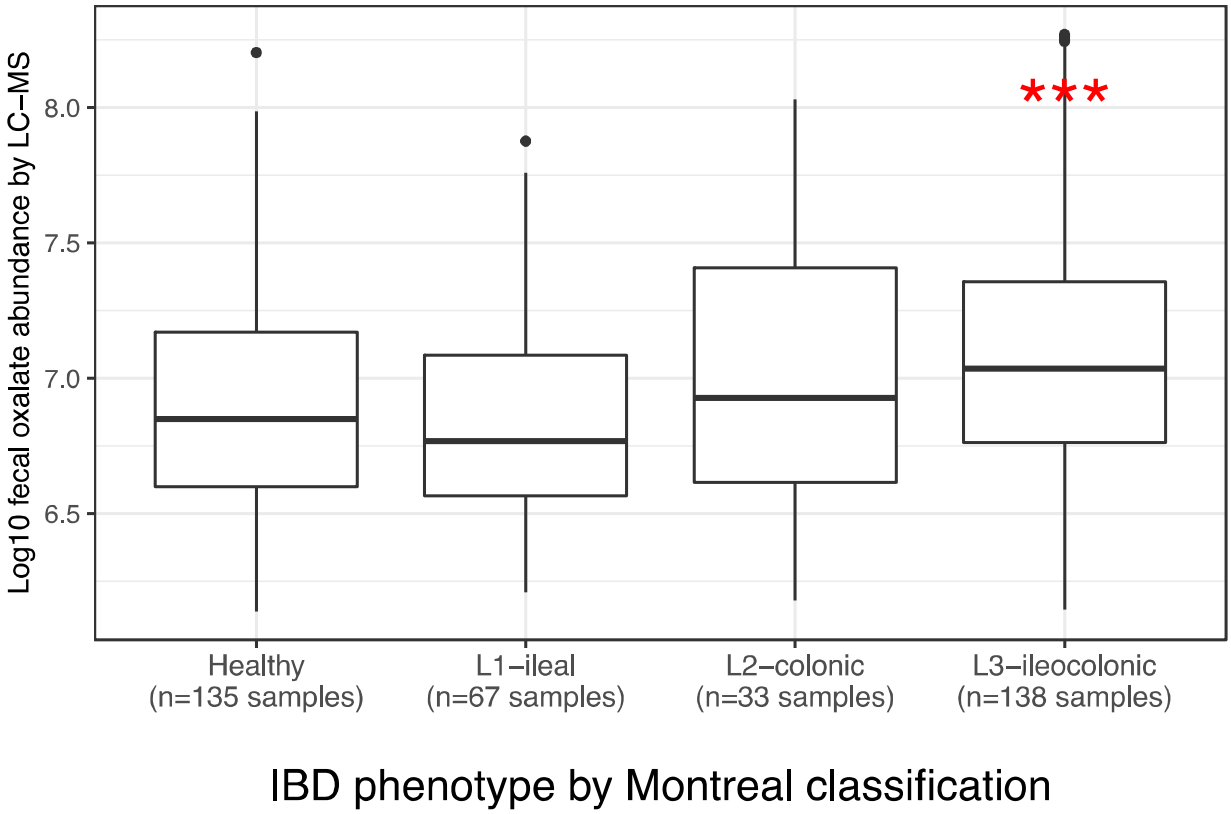

606

607

608

609 **Figure S9.** Fecal oxalate concentrations in CD patients, according to the Montreal clinical classification.
610 ***$p < 0.001$ by Mann-Whitney test.

611

612 **Figure S10**

613 **A**

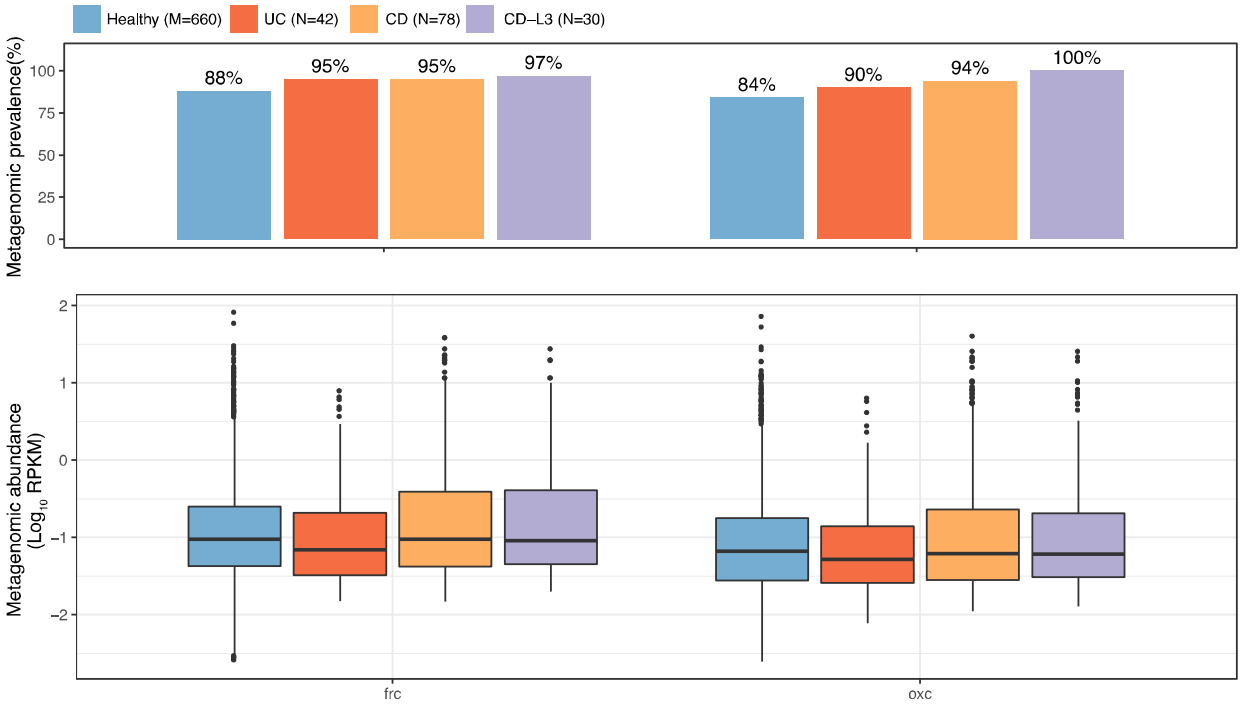

614

615 **B**

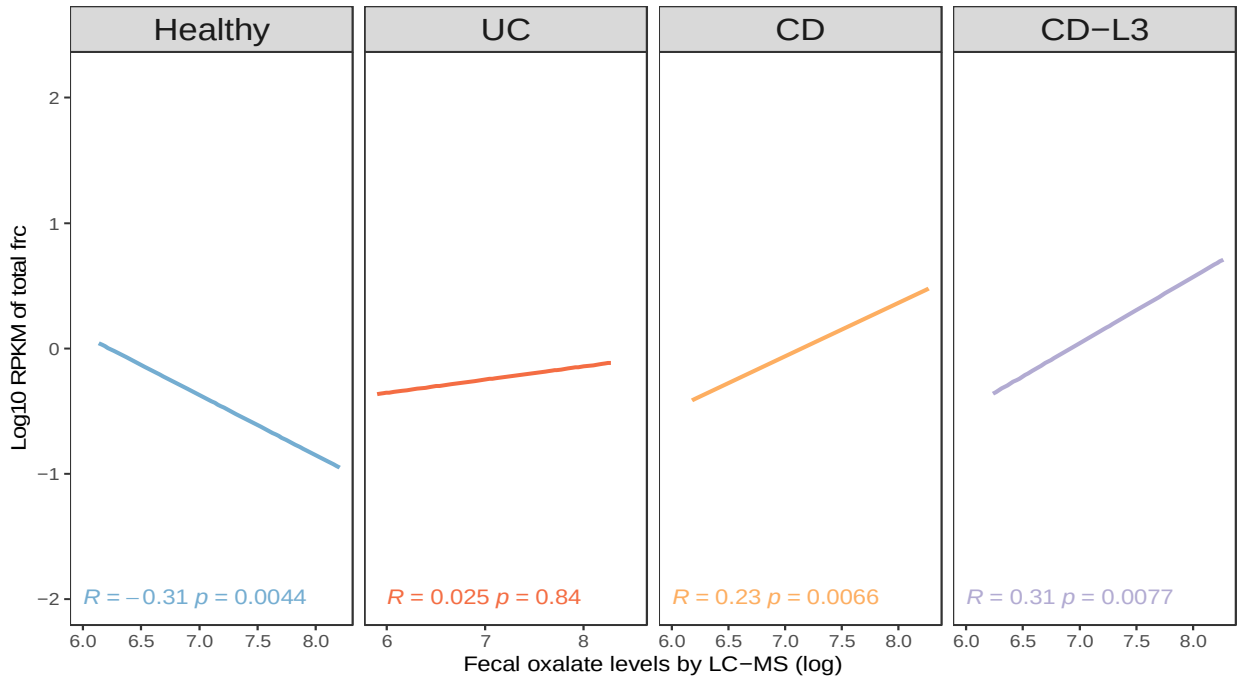

616

617

618 **Figure S10**. **(A)** Metagenomic prevalence (top) and abundance (bottom) of *frc* and *oxc* in healthy, UC,
619 CD, and CD-L3 subjects. **(B)** Spearman correlation of fecal oxalate and total metagenomic OXC
620 abundance.

References

1. Ruiz-Agudo, E., et al., *A non-classical view on calcium oxalate precipitation and the role of citrate.* Nat Commun, 2017. **8**(1): p. 768.
2. Asplin, J., et al., *Supersaturation and stone composition in a network of dispersed treatment sites.* J Urol., 1998. **159**(6): p. 1821-1825.
3. Beck, B.B., et al., *Hyperoxaluria and systemic oxalosis: an update on current therapy and future directions.* Expert Opin Investig Drugs, 2013. **22**(1): p. 117-29.
4. Mookadam, F., et al., *Cardiac abnormalities in primary hyperoxaluria.* Circ J, 2010. **74**(11): p. 2403-9.
5. Punjabi, O.S., K. Riaz, and M.B. Mets, *Crystalline retinopathy in primary hyperoxaluria.* J AAPOS, 2011. **15**(2): p. 214-6.
6. Lieske, J.C., et al., *Stone composition as a function of age and sex.* Clin J Am Soc Nephrol, 2014. **9**(12): p. 2141-6.
7. Stamatelou, K.K., et al., *Time trends in reported prevalence of kidney stones in the United States: 1976-1994.* Kidney Int, 2003. **63**(5): p. 1817-23.
8. Scales, C.D., et al., *Prevalence of kidney stones in the United States.* Eur Urol, 2012. **62**(1): p. 160-5.
9. Rule, A.D., et al., *The ROKS nomogram for predicting a second symptomatic stone episode.* J Am Soc Nephrol, 2014. **25**(12): p. 2878-86.
10. Scales, C.D., Jr., et al., *Prevalence of kidney stones in the United States.* Eur Urol, 2012. **62**(1): p. 160-5.
11. Knauf, F., et al., *NALP3-mediated inflammation is a principal cause of progressive renal failure in oxalate nephropathy.* Kidney Int, 2013. **84**(5): p. 895-901.
12. Mulay, S.R., et al., *Oxalate-induced chronic kidney disease with its uremic and cardiovascular complications in C57BL/6 mice.* Am J Physiol Renal Physiol, 2016. **310**(8): p. F785-F795.
13. Waikar, S.S., et al., *Association of Urinary Oxalate Excretion With the Risk of Chronic Kidney Disease Progression.* JAMA Intern Med, 2019.
14. Mulay, S.R., et al., *Calcium oxalate crystals induce renal inflammation by NLRP3-mediated IL-1beta secretion.* J Clin Invest, 2013. **123**(1): p. 236-46.
15. Barber, H.H. and E.J. Gallimore, *The metabolism of oxalic acid in the animal body.* Biochem J, 1940. **34**(2): p. 144-8.
16. Allison, M.J., et al., *Oxalate degradation by gastrointestinal bacteria from humans.* J Nutr, 1986. **116**(3): p. 455-60.
17. Allison, M.J. and H.M. Cook, *Oxalate degradation by microbes of the large bowel of herbivores: the effect of dietary oxalate.* Science, 1981. **212**(4495): p. 675-676.
18. Allison, M.J., E.T. Littledike, and L.F. James, *Changes in ruminal oxalate degradation rates associated with adaptation to oxalate ingestion.* J Anim Sci., 1977. **45**(5): p. 1173-1179.
19. Tasian, G.E., et al., *Oral Antibiotic Exposure and Kidney Stone Disease.* J Am Soc Nephrol, 2018.
20. Ferraro, P.M., et al., *Antibiotic Use and Risk of Incident Kidney Stones in Female Nurses.* Am J Kidney Dis, 2019.
21. Nazzal, L. and M.J. Blaser, *Does the Receipt of Antibiotics for Common Infectious Diseases Predispose to Kidney Stones? A Cautionary Note for All Health Care Practitioners.* J Am Soc Nephrol, 2018. **29**(6): p. 1590-1592.
22. Abratt, V.R. and S.J. Reid, *Oxalate-degrading bacteria of the human gut as probiotics in the management of kidney stone disease.* Adv Appl Microbiol, 2010. **72**: p. 63-87.
23. Allison, M.J., et al., *Oxalobacter formigenes gen. nov., sp. nov.: oxalate-degrading anaerobes that inhabit the gastrointestinal tract.* Arch Microbiol, 1985. **141**(1): p. 1-7.

24. Dawson, K.A., M.J. Allison, and P.A. Hartman, *Isolation and some characteristics of anaerobic oxalate-degrading bacteria from the rumen.* Applied and environmental microbiology, 1980. **40**(4): p. 833-839.
25. Ruan, Z.-S., et al., *Identification, purification, and reconstitution of OxlT, the oxalate: formate antiport protein of Oxalobacter formigenes.* Journal of Biological Chemistry, 1992. **267**(15): p. 10537-10543.
26. Lung, H.-y., J.G. Cornelius, and A.B. Peck, *Cloning and expression of the oxalyl-CoA decarboxylase gene from the bacterium, Oxalobacter formigenes: prospects for gene therapy to control Ca-oxalate kidney stone formation.* American journal of kidney diseases, 1991. **17**(4): p. 381-385.
27. Baetz, A.L. and M.J. Allison, *Purification and characterization of formyl-coenzyme A transferase from Oxalobacter formigenes.* Journal of bacteriology, 1990. **172**(7): p. 3537-3540.
28. Hoppe, B., et al., *Efficacy and safety of Oxalobacter formigenes to reduce urinary oxalate in primary hyperoxaluria.* Nephrol Dial Transplant, 2011. **26**(11): p. 3609-15.
29. Hoppe, B., et al., *A randomised Phase I/II trial to evaluate the efficacy and safety of orally administered Oxalobacter formigenes to treat primary hyperoxaluria.* Pediatr Nephrol, 2017. **32**(5): p. 781-790.
30. Hatch, M. and R.W. Freel, *A human strain of Oxalobacter (HC-1) promotes enteric oxalate secretion in the small intestine of mice and reduces urinary oxalate excretion.* Urolithiasis, 2013. **41**(5): p. 379-84.
31. Arvans, D., et al., *Oxalobacter formigenes-Derived Bioactive Factors Stimulate Oxalate Transport by Intestinal Epithelial Cells.* J Am Soc Nephrol, 2017. **28**(3): p. 876-887.
32. Li, X., M.L. Ellis, and J. Knight, *Oxalobacter formigenes Colonization and Oxalate Dynamics in a Mouse Model.* Applied and Environmental Microbiology, 2015. **81**(15): p. 5048-5054.
33. Li, X., et al., *Response of Germfree Mice to Colonization by Oxalobacter formigenes and Altered Schaedler Flora.* Applied and environmental microbiology, 2016. **82**(23): p. 6952-6960.
34. Azcarate-Peril, M.A., et al., *Transcriptional and functional analysis of oxalyl-coenzyme A (CoA) decarboxylase and formyl-CoA transferase genes from Lactobacillus acidophilus.* Appl Environ Microbiol, 2006. **72**(3): p. 1891-9.
35. Turroni, S., et al., *Oxalate consumption by lactobacilli: evaluation of oxalyl-CoA decarboxylase and formyl-CoA transferase activity in Lactobacillus acidophilus.* J Appl Microbiol, 2007. **103**(5): p. 1600-9.
36. Lewanika, T.R., et al., *Lactobacillus gasseri Gasser AM63(T) degrades oxalate in a multistage continuous culture simulator of the human colonic microbiota.* FEMS Microbiol Ecol, 2007. **61**(1): p. 110-20.
37. Ferraz, R.R., et al., *Effects of Lactobacillus casei and Bifidobacterium breve on urinary oxalate excretion in nephrolithiasis patients.* Urol Res, 2009. **37**(2): p. 95-100.
38. Kolandaswamy, A., L. George, and S. Sadasivam, *Heterologous expression of oxalate decarboxylase in Lactobacillus plantarum NC8.* Curr Microbiol, 2009. **58**(2): p. 117-21.
39. Sasikumar, P., et al., *Secretion of biologically active heterologous oxalate decarboxylase (OxdC) in Lactobacillus plantarum WCFS1 using homologous signal peptides.* Biomed Res Int, 2013. **2013**: p. 280432.
40. Miller, A.W., K.D. Kohl, and M.D. Dearing, *The Gastrointestinal Tract of the White-Throated Woodrat (Neotoma albigula) Harbors Distinct Consortia of Oxalate-Degrading Bacteria.* Applied and Environmental Microbiology, 2014. **80**(5): p. 1595-1601.
41. Kullin, B., et al., *A functional analysis of the formyl-coenzyme A (frc) gene from Lactobacillus reuteri 100-23C.* J Appl Microbiol, 2014. **116**(6): p. 1657-67.
42. Turroni, S., et al., *Oxalate-degrading activity in Bifidobacterium animalis subsp. lactis: impact of acidic conditions on the transcriptional levels of the oxalyl coenzyme A (CoA) decarboxylase and formyl-CoA transferase genes.* Appl Environ Microbiol, 2010. **76**(16): p. 5609-20.

43. Klimesova, K., J.M. Whittamore, and M. Hatch, *Bifidobacterium animalis subsp. lactis decreases urinary oxalate excretion in a mouse model of primary hyperoxaluria.* Urolithiasis, 2015. **43**(2): p. 107-17.
44. McConnell, N., et al., *Risk factors for developing renal stones in inflammatory bowel disease.* BJU Int, 2002. **89**(9): p. 835-41.
45. Corica, D. and C. Romano, *Renal Involvement in Inflammatory Bowel Diseases.* J Crohns Colitis, 2016. **10**(2): p. 226-35.
46. Liu, M. and L. Nazzal, *Enteric hyperoxaluria: role of microbiota and antibiotics.* Curr Opin Nephrol Hypertens, 2019. **28**(4): p. 352-359.
47. Daniel, S.L., C. Pilsl, and H.L. Drake, *Oxalate metabolism by the acetogenic bacterium Moorella thermoacetica.* FEMS Microbiol Lett, 2004. **231**(1): p. 39-43.
48. Pierce, E., D.F. Becker, and S.W. Ragsdale, *Identification and characterization of oxalate oxidoreductase, a novel thiamine pyrophosphate-dependent 2-oxoacid oxidoreductase that enables anaerobic growth on oxalate.* J Biol Chem, 2010. **285**(52): p. 40515-24.
49. Allison, M.J., et al., *Oxalobacter formigenes gen. nov., sp. nov.: oxalate-degrading anaerobes that inhabit the gastrointestinal tract.* Arch.Microbiol., 1985. **141**(1): p. 1-7.
50. Blackmore, M.A. and J.R. Quayle, *Microbial growth on oxalate by a route not involving glyoxylate carboligase.* Biochem J, 1970. **118**(1): p. 53-9.
51. Dumas, B., et al., *Identification of barley oxalate oxidase as a germin-like protein.* C R Acad Sci III, 1993. **316**(8): p. 793-8.
52. Anand, R., et al., *Structure of oxalate decarboxylase from Bacillus subtilis at 1.75 A resolution.* Biochemistry, 2002. **41**(24): p. 7659-69.
53. Foster, J., et al., *A previously unknown oxalyl-CoA synthetase is important for oxalate catabolism in Arabidopsis.* Plant Cell, 2012. **24**(3): p. 1217-29.
54. Moussatche, P., et al., *Characterization of Ceriporiopsis subvermispora bicupin oxalate oxidase expressed in Pichia pastoris.* Arch Biochem Biophys, 2011. **509**(1): p. 100-7.
55. Moomaw, E.W., et al., *Kinetic and spectroscopic studies of bicupin oxalate oxidase and putative active site mutants.* PLoS One, 2013. **8**(3): p. e57933.
56. Moomaw, E.W., R. Uberto, and C. Tu, *Membrane inlet mass spectrometry reveals that Ceriporiopsis subvermispora bicupin oxalate oxidase is inhibited by nitric oxide.* Biochem Biophys Res Commun, 2014. **450**(1): p. 750-4.
57. Rana, H., et al., *Isothermal titration calorimetry uncovers substrate promiscuity of bicupin oxalate oxidase from Ceriporiopsis subvermispora.* Biochem Biophys Rep, 2016. **5**: p. 396-400.
58. Burrell, M.R., et al., *Oxalate decarboxylase and oxalate oxidase activities can be interchanged with a specificity switch of up to 282,000 by mutating an active site lid.* Biochemistry, 2007. **46**(43): p. 12327-36.
59. Mitchell, A.L., et al., *InterPro in 2019: improving coverage, classification and access to protein sequence annotations.* Nucleic Acids Res, 2019. **47**(D1): p. D351-D360.
60. Mulder, N.J., et al., *InterPro, progress and status in 2005.* Nucleic Acids Res, 2005. **33**(Database issue): p. D201-5.
61. Buchfink, B., C. Xie, and D.H. Huson, *Fast and sensitive protein alignment using DIAMOND.* Nat Methods, 2015. **12**(1): p. 59-60.
62. Fontenot, E.M., et al., *YfdW and YfdU are required for oxalate-induced acid tolerance in Escherichia coli K-12.* J Bacteriol, 2013. **195**(7): p. 1446-55.
63. Cho, J.G., et al., *Assessment of in vitro oxalate degradation by Lactobacillus species cultured from veterinary probiotics.* Am J Vet Res, 2015. **76**(9): p. 801-6.
64. Mogna, L., et al., *Screening of different probiotic strains for their in vitro ability to metabolise oxalates: any prospective use in humans?* J Clin Gastroenterol, 2014. **48 Suppl 1**: p. S91-5.
65. Gruez, A., et al., *The crystal structure of the Escherichia coli YfdW gene product reveals a new fold of two interlaced rings identifying a wide family of CoA transferases.* J Biol Chem, 2003. **278**(36): p. 34582-6.

66. Federici, F., et al., *Characterization and heterologous expression of the oxalyl coenzyme A decarboxylase gene from Bifidobacterium lactis.* Appl Environ Microbiol, 2004. **70**(9): p. 5066-73.
67. Cornick, N.A. and M.J. Allison, *Assimilation of oxalate, acetate, and CO2 by Oxalobacter formigenes.* Can J Microbiol, 1996. **42**(11): p. 1081-6.
68. Allison, M.J., et al., *Oxalate degradation by gastrointestinal bacteria from humans.* J Nutr., 1986. **116**(3): p. 455-460.
69. Barnett, C., et al., *The presence of Oxalobacter formigenes in the microbiome of healthy young adults.* The Journal of urology, 2016. **195**(2): p. 499-506.
70. Liu, M., et al., *Oxalobacter formigenes-associated host features and microbial community structures examined using the American Gut Project.* Microbiome, 2017. **5**(1): p. 108.
71. Kelly, J.P., et al., *Factors related to colonization with Oxalobacter formigenes in U.S. adults.* J Endourol, 2011. **25**(4): p. 673-9.
72. PeBenito, A., et al., *Comparative prevalence of Oxalobacter formigenes in three human populations.* Sci Rep, 2019. **9**(1): p. 574.
73. Cury, D.B., A.C. Moss, and N. Schor, *Nephrolithiasis in patients with inflammatory bowel disease in the community.* Int J Nephrol Renovasc Dis, 2013. **6**: p. 139-42.
74. Franzosa, E.A., et al., *Gut microbiome structure and metabolic activity in inflammatory bowel disease.* Nat Microbiol, 2019. **4**(2): p. 293-305.
75. Lloyd-Price, J., et al., *Multi-omics of the gut microbial ecosystem in inflammatory bowel diseases.* Nature, 2019. **569**(7758): p. 655-662.
76. Daniel, S.L., P.A. Hartman, and M.J. Allison, *Intestinal colonization of laboratory rats with Oxalobacter formigenes.* Appl.Environ.Microbiol., 1987. **53**(12): p. 2767-2770.
77. Daniel, S.L., P.A. Hartman, and M.J. Allison, *Microbial degradation of oxalate in the gastrointestinal tracts of rats.* Appl.Environ.Microbiol., 1987. **53**(8): p. 1793-1797.
78. Ticinesi, A., A. Nouvenne, and T. Meschi, *Gut microbiome and kidney stone disease: not just an Oxalobacter story.* Kidney Int, 2019. **96**(1): p. 25-27.
79. Miller, A.W., et al., *Inhibition of urinary stone disease by a multi-species bacterial network ensures healthy oxalate homeostasis.* Kidney Int, 2019. **96**(1): p. 180-188.
80. Ticinesi, A., et al., *Understanding the gut-kidney axis in nephrolithiasis: an analysis of the gut microbiota composition and functionality of stone formers.* Gut, 2018. **67**(12): p. 2097-2106.
81. Stern, J.M., et al., *Evidence for a distinct gut microbiome in kidney stone formers compared to non-stone formers.* Urolithiasis, 2016. **44**(5): p. 399-407.
82. Ellis, M.E., et al., *Proteome Dynamics of the Specialist Oxalate Degrader Oxalobacter formigenes.* J Proteomics Bioinform, 2016. **9**(1): p. 19-24.
83. Halbritter, J., et al., *Fourteen monogenic genes account for 15% of nephrolithiasis/nephrocalcinosis.* J Am Soc Nephrol, 2015. **26**(3): p. 543-51.
84. Hylander, E., S. Jarnum, and I. Frandsen, *Urolithiasis and hyperoxaluria in chronic inflammatory bowel disease.* Scand J Gastroenterol, 1979. **14**(4): p. 475-9.
85. Hylander, E., et al., *Enteric hyperoxaluria: dependence on small intestinal resection, colectomy, and steatorrhoea in chronic inflammatory bowel disease.* Scand J Gastroenterol, 1978. **13**(5): p. 577-88.
86. Hoppe, B., et al., *Oxalobacter formigenes: a potential tool for the treatment of primary hyperoxaluria type 1.* Kidney Int, 2006. **70**(7): p. 1305-11.
87. Hoppe, B., et al., *Oxalate degrading bacteria: new treatment option for patients with primary and secondary hyperoxaluria?* Urological Research, 2005. **33**(5): p. 372-375.
88. Canales, B.K. and M. Hatch, *Oxalobacter formigenes colonization normalizes oxalate excretion in a gastric bypass model of hyperoxaluria.* Surg Obes Relat Dis, 2017. **13**(7): p. 1152-1157.
89. Hatch, M., et al., *Oxalobacter sp. reduces urinary oxalate excretion by promoting enteric oxalate secretion.* Kidney Int, 2006. **69**(4): p. 691-8.

90. Li, J., et al., *An integrated catalog of reference genes in the human gut microbiome.* Nat Biotechnol, 2014. **32**(8): p. 834-41.
91. Ehrlich, S.D., *MetaHIT: The European Union Project on Metagenomics of the Human Intestinal Tract*, in *Metagenomics of the Human Body*, K.E. Nelson, Editor. 2011, Springer New York: New York, NY. p. 307-316.
92. Franzosa, E.A., et al., *Relating the metatranscriptome and metagenome of the human gut.* Proc Natl Acad Sci U S A, 2014. **111**(22): p. E2329-38.
93. Petersen, L.M., et al., *Community characteristics of the gut microbiomes of competitive cyclists.* Microbiome, 2017. **5**(1): p. 98.
94. Abu-Ali, G.S., et al., *Metatranscriptome of human faecal microbial communities in a cohort of adult men.* Nat Microbiol, 2018. **3**(3): p. 356-366.
95. Schirmer, M., et al., *Dynamics of metatranscription in the inflammatory bowel disease gut microbiome.* Nat Microbiol, 2018. **3**(3): p. 337-346.
96. Franzosa, E.A., et al., *Species-level functional profiling of metagenomes and metatranscriptomes.* Nat Methods, 2018. **15**(11): p. 962-968.
97. Graz, M., et al., *Oxalic acid degradation by a novel fungal oxalate oxidase from Abortiporus biennis.* Acta Biochim Pol, 2016. **63**(3): p. 595-600.
98. Kumar, R., V. Hooda, and C.S. Pundir, *Purification and partial characterization of oxalate oxidase from leaves of forage Sorghum (Sorghum vulgare var. KH-105) seedlings.* Indian J Biochem Biophys, 2011. **48**(1): p. 42-6.
99. Svedruzic, D., et al., *Investigating the roles of putative active site residues in the oxalate decarboxylase from Bacillus subtilis.* Arch Biochem Biophys, 2007. **464**(1): p. 36-47.
100. Just, V.J., et al., *A closed conformation of Bacillus subtilis oxalate decarboxylase OxdC provides evidence for the true identity of the active site.* J Biol Chem, 2004. **279**(19): p. 19867-74.
101. Tanner, A., et al., *Oxalate decarboxylase requires manganese and dioxygen for activity. Overexpression and characterization of Bacillus subtilis YvrK and YoaN.* J Biol Chem, 2001. **276**(47): p. 43627-34.
102. Edgar, R.C., *MUSCLE: multiple sequence alignment with high accuracy and high throughput.* Nucleic Acids Res, 2004. **32**(5): p. 1792-7.
103. Gouy, M., S. Guindon, and O. Gascuel, *SeaView version 4: A multiplatform graphical user interface for sequence alignment and phylogenetic tree building.* Mol Biol Evol, 2010. **27**(2): p. 221-4.
104. Charif, D., et al., *Online synonymous codon usage analyses with the ade4 and seqinR packages.* Bioinformatics, 2005. **21**(4): p. 545-7.
105. Fitch, W.M., *An improved method of testing for evolutionary homology.* J Mol Biol, 1966. **16**(1): p. 9-16.
106. Kurtz, Z.D., et al., *Sparse and Compositionally Robust Inference of Microbial Ecological Networks.* PLOS Computational Biology, 2015. **11**(5): p. e1004226.